Available online at www.sciencedirect.com
SCIENCE DIRECT®
Inorganic Chemistry Communications 6 (2003) 670–674
INORGANIC CHEMISTRY COMMUNICATIONS
www.elsevier.com/locate/inoche

The synthesis and characterization of $Pb_5S_2I_6$ whiskers and tubules

Qing Yang, Kaibin Tang *, Chunrui Wang, Jian Zuo, Yitai Qian

Department of Chemistry and Structure Research Laboratory, University of Science and Technology of China, Hefei, Anhui 230026, China

Received 18 December 2002; accepted 4 March 2003

Abstract

$Pb_5S_2I_6$ whiskers and tubules were synthesized from the reaction among lead chloride, thiourea, and excess sodium iodide under hydrothermal conditions at 200 °C for 20–40 h. XRD, SEM, XPS, ICP-AES, and TEM characterized the final products. Most products are whiskers with structure of 3–4 mm in length, 0.5–2.0 μm in diameter for a singular one. Meanwhile, about 10% tubules are produced in the process. The tubules are 3–6 mm in length, 8–20 μm in diameter, and 1–3 μm in thickness. Nanowhiskers were also produced in the route at 180–200 °C for 8–10 h. Raman spectra show that the $Pb_5S_2I_6$ crystals have complex vibrational modes of PbS and PbI_2.

PACS: 61.10.N; 61.66.F; 61.72.

Keywords: Chalcogenide halides; Crystals; Hydrothermal reaction; X-ray photoelectron spectroscopy; Raman spectroscopy

1. Introduction

Chalcogenide halides are a group of important solid-state materials having many interesting properties such as high conductivity, photoconductivity, ferroelectricity, and piezoelectricity [1–4]. Owing to their novel properties having possible potential applications and possessing technological importance, chalcogenide halides have excited growing interest in the scientific world during the past several decades [5–10]. $Pb_5S_2I_6$ as an important IV–V–VI chalcogenide halide compound was first synthesized by heating the mixture of PbS and PbI_2 at 350 °C in 1968 [11]. The phase diagram of the PbS–PbI_2 was investigated by X-ray diffraction and DTA methods [12]. Thereafter, the crystallization conditions of $Pb_5S_2I_6$ in the system Pb–S–I–R–H_2O (R being a solvent) have been investigated by Popolitov and co-workers [13–16]. Meanwhile, the dielectric and photosemiconducting properties of the $Pb_5S_2I_6$ crystals were also studied [17,18]. More recently, iodide-doped lead sulfide crystals have been developed as semiconducting sensors for determining nitrogen oxides (NO, NO2) [19].

Currently, both one-dimensional (1D) materials and three-dimensional (3D) mesoscale tubular ones have attracted great attention because of their potential application in microscopic research and the development of devices. Meanwhile, hydrothermal synthesis as a versatile synthetic technique has been intensively employed to prepare inorganic materials including single crystals and nanocrystals. With this method, we have successfully synthesized several different chalcogenide (including tubular) crystals [20,21]. Based on our recent researches, we first obtained the tubular $Pb_5S_2I_6$ crystals from a hydrothermal reaction of iodine disproportionation [22]. Compared with the reaction among Pb, S, I_2, and HI at above 300 °C [14], the reaction we reported is moderate. In order to extend the synthesis of tubular crystals and to investigate the properties, we reported the preparation of the $Pb_5S_2I_6$ whiskers and tubular crystals under hydrothermal reaction from iodide I-source at 200 °C and measure the crystals by Raman spectroscopy in the present paper.

* Corresponding author. Tel.: +86-551-3601600; fax: +86-551-3601600.
E-mail addresses: qyoung@ustc.edu.cn (Q. Yang), kbtang@ustc.edu.cn (K. Tang).

1387-7003/03/$ - see front matter © 2003 Elsevier Science B.V. All rights reserved.
doi:10.1016/S1387-7003(03)00084-4

2. Experimental

2.1. Synthesis

$Pb_5S_2I_6$ crystals were synthesized in a Teflon-lined stainless steel autoclave through the hydrothermal synthetic route. In a typical experiment, an appropriate amount of analytically pure $PbCl_2$ (1.0 g), $(NH_2)_2CS$ and NaI (with a molar ratio of 5:2:6–12) was added into the Teflon-lined autoclave, which was filled up to 90% of the total volume (50 ml) with distilled water. Then, the autoclave was maintained at 200 °C for 20–40 h and cooled to room temperature, naturally. The as-prepared precipitates were filtrated, washed with carbon disulfide, distilled water, and absolute ethanol several times to remove byproducts. After drying in a vacuum at 60–70 °C for 2 h, the samples in orange red color were obtained.

2.2. Characterization of products

The products were determined by X-ray diffraction (XRD) operated on a Chain Dandong rotating anode X-ray diffractometer with graphite monochromatized Cu Kα radiation ($\lambda = 1.54178$ Å). The scanning rate of 0.060°/s was applied to record the patterns in the 2θ range of 10–60°. The morphology of the crystals was observed by scanning electron microscopy (SEM), which was performed on a Hitachi X-650 scanning electron microanalyzer. The verification of product formation was obtained by X-ray photoelectron spectra (XPS), which was collected on an ESCALAB MK II X-rays photoelectron spectrometer by using nonmonochromatized Mg Kα X-ray as the excitation source. Meanwhile, elemental analysis was done by ICP-AES, which was carried on an Atomscan Advantage (Thermo Jarrell Ash Corporation). Transmission electron microscopy (TEM) photographs were taken with a Hitachi Model H-800 transmission electron microscope, using an accelerating voltage of 200 kV. The samples for these measurements were dispersed in absolute ethanol with arc ultrasonic generator and then the solutions were dropped onto copper grids coated with amorphous carbon films. Raman spectra of the samples were recorded on a Spex 1403 Raman spectrometer with 514.5 nm excitation lines, which were recorded at ambient temperature. The spectra were obtained in the range 40–800 cm^{-1} at a laser power of 150 mW with slit of 140 μm (~1 cm^{-1}) and an integration time of 0.5 s per step.

3. Results and discussion

In our hydrothermal synthetic route, the $Pb_5S_2I_6$ whiskers and tubules were achieved from the reaction change among lead chloride, thiourea, and excess sodium iodide at a moderate temperature. The formation of the products may be proposed as follows:

$$(NH_2)_2CS + 2H_2O \rightarrow H_2S + CO_2 + 2NH_3 \quad (1)$$

$$PbCl_2 + H_2S \rightarrow PbS + 2HCl \quad (2)$$

$$PbCl_2 + 2NaI \rightarrow PbI_2 + 2NaCl \quad (3)$$

$$2PbS + 3PbI_2 \rightarrow Pb_5S_2I_6 \quad (4)$$

$$HCl + NH_3 \rightarrow NH_4^+ + Cl^- \quad (5)$$

In these procedures, PbS was first formed, which could be detected in a short reactive period (2 h). The early-formed PbS provides a nucleus for subsequent combination with PbI_2 in (4) for the formation of the $Pb_5S_2I_6$ crystals. Reaction (5) is the one for by-products.

Fig. 1 shows the X-ray diffraction (XRD) patterns of the polycrystalline powder ground from the products. The XRD spectra could be indexed to the monoclinic $Pb_5S_2I_6$ phase with lattice parameters $a = 14.333$, $b = 4.432$, $c = 14.529$, and $\beta = 98.0°$, which are in agreement with the reported data for $Pb_5S_2I_6$ [12]. No other characteristic peaks of impurities such as PbS or S were observed. The peaks of by-products of NaCl or NH_4Cl were not obviously observed in the spectra.

The scanning electron microscopy (SEM) images of as-grown $Pb_5S_2I_6$ crystals are shown in Fig. 2. It can be seen that the morphologies of $Pb_5S_2I_6$ crystals are rod-like whiskers (Fig. 2(a)). Typically, the structure is 3–4 mm in length, 0.5–2.0 μm in diameter for a singular crystal. With further observation, some larger crystals have hollow structure. Electron microscope images of the samples reveal that the tubules are about 10% in the total yield. The tubules are 3–6 mm in length, 8–20 μm in diameter, and 1–3 μm in thickness (Figs. 2(b–c)). Fig. 2(b) shows a tubule with thin wall, whereas Fig. 2(c) shows one with thick wall. Comparing with our previous synthesis [22], we obtained similar tubular crystals from

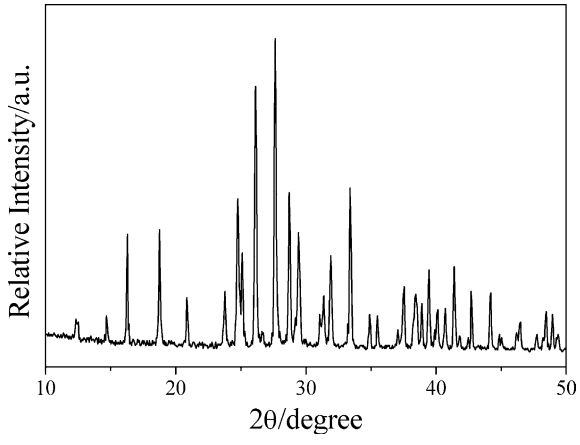

Fig. 1. Powder X-ray diffraction (XRD) patterns of $Pb_5S_2I_6$ products.

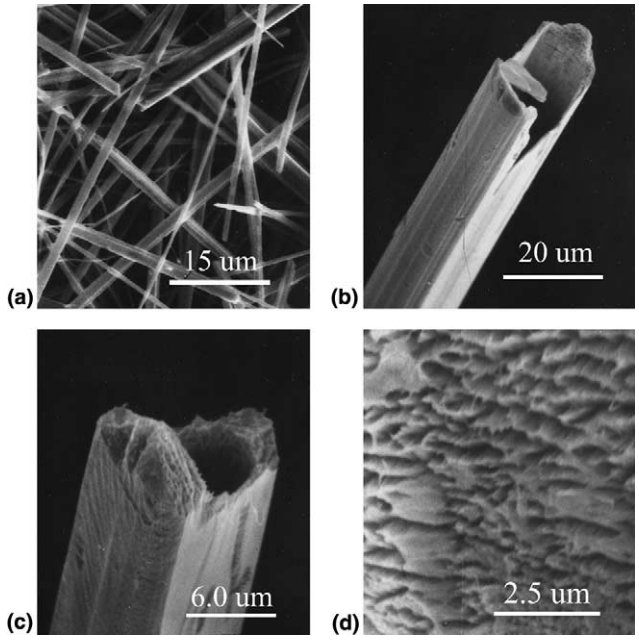

Fig. 2. SEM images of the as-produced $Pb_5S_2I_6$ crystals. (a) The low-magnification image of the crystals. (b–c) The typical images of the tubular crystals. (d) The end surface of a crystal with some minute hollows.

the different reagents. We could conclude that the morphology of the whiskers is mainly caused by the anisotropies and the different growth speeds of crystal plane. In the route, the tubules may be formed from some hollow nucleus. Fig. 2(d) is a SEM image of an end surface of a crystal. It is observed that the surface is not even and it contains some hollow structures, which could serve as the hollow nucleus to form tubules in the epitaxial growth along axial direction.

To provide evidence for the formation of the $Pb_5S_2I_6$ crystals, XPS was employed to analyze the obtained products. Fig. 3(a) is the survey spectra of samples obtained in the process. From the spectra, the XPS results show that the presence of Pb, S, and I from the binding energies, which are consistent with the formation of $Pb_5S_2I_6$. The close-up spectrum of Pb was shown in Fig. 3(b) and the obtained value of the binding energy for Pb $4f_{7/2}$ is 139.45 eV, which is near to the binding energy of Pb $4f_{7/2}$ in $PbSO_4$ [23]. Fig. 3(c) is the spectra for S 2p (161.50 eV) core, which shows that no elemental sulphur (164.00 eV) [24] was observed in the as-produced $Pb_5S_2I_6$ crystals. The broadened peak of S 2p may show the two coordination states of S^{2-} in the crystals. Elemental iodine was also analyzed by XPS and the close-up spectra show the binding energy for I $3d_{5/2}$ is 620.20 eV (shown in Fig. 3(d)). The value is close to the reported value for I $3d_{5/2}$ (620.50 eV) in $Rb_3Sb_2I_9$ [25]. Elemental analysis was employed to analyze the composition of as-prepared products by ICP-AES and the results revealed that the obtained $Pb_5S_2I_6$ crystals are close to stoichiometry.

Conditions of the reaction system were investigated in the experiments. The pH value of reaction system mainly affects the formation and the morphology of the $Pb_5S_2I_6$ crystals. The acidic condition is favorable for the growth of the $Pb_5S_2I_6$ crystals. On one hand, acid condition is favorable for the transition of Pb^{2+} from PbS to $Pb_5S_2I_6$, and on the other hand, the acidic condition promotes the formation of the tubular crystals because the soluble effect of acid could form nucleus with hollow structure. Otherwise, PbS is predominated in the products in basic conditions from the experiments. In our previous synthesis [22], the acidic conditions were obtained by the I_2 disproportionation under hydrothermal conditions. In the present route, it may be adjusted by dropping 2–5 ml of 5% HCl in solution if it is necessary. When we did not drop acid into the system, the yield of the tubules was not more than 10%. When we dropped HCl into the system down to pH less than 3, the yield of the tubules had about a half time increase. It is noted that over acidic condition (pH less than 1) will make the crystals become irregular. According to phase diagram of Pb–S–I–R–H_2O, reaction temperature is also a critical factor to the formation of $Pb_5S_2I_6$. When temperature was less than 160 °C, the products could not be well crystallized. Other factors such as the reagents and the feedstock may affect the products and the yield in the experiments. S-sources of Na_2S and $(NH_4)_2S$ were also used to synthesize the target crystals in the route. These basic S-sources are unfriendly for the formation of $Pb_5S_2I_6$ crystals unless an acidic condition is adjusted (by adding HCl into the reaction system). Based on the investigation from the experiments, it could be concluded that the anisotropic 1D crystal growth is the intrinsic growth nature of the monoclinic $Pb_5S_2I_6$, while the hollow structure of the crystals could be obtained by altering the growth conditions. In the route, $Pb_5S_2I_6$ nanowhiskers with 50–300 nm in diameter and more than 10 μm in length were also synthesized among $PbCl_2$, $(NH_2)_2CS$ and NaI at 180–200 °C for 8–10 h (Fig. 4).

The Raman spectra of the samples obtained in the process are shown in Fig. 5. Although the spectra of $Pb_5S_2I_6$ have not been reported before in the literature, $Pb_5S_2I_6$ could be considered as a complex system as PbS–PbI_2 generally. That is, they could be shown as the complex behaviors of the two vibrational modes of PbS and PbI_2 in Raman spectroscopy. The intense peak locating at 133 cm^{-1} (Fig. 5(a)) could be signed as the lattice mode vibration for PbS [26]. The broad peak observed at 270 cm^{-1} could be attributed to two-phonon process in PbS [27]. The weak broad band observed at about 435 cm^{-1} could be assigned to the first overtones of the LO phonon mode for PbS according to the literature [28]. Meanwhile, the acoustic modes of PbS have been observed at 46 and 62 cm^{-1} [27b]. However, owing to the differences between PbS and $Pb_5S_2I_6$, the

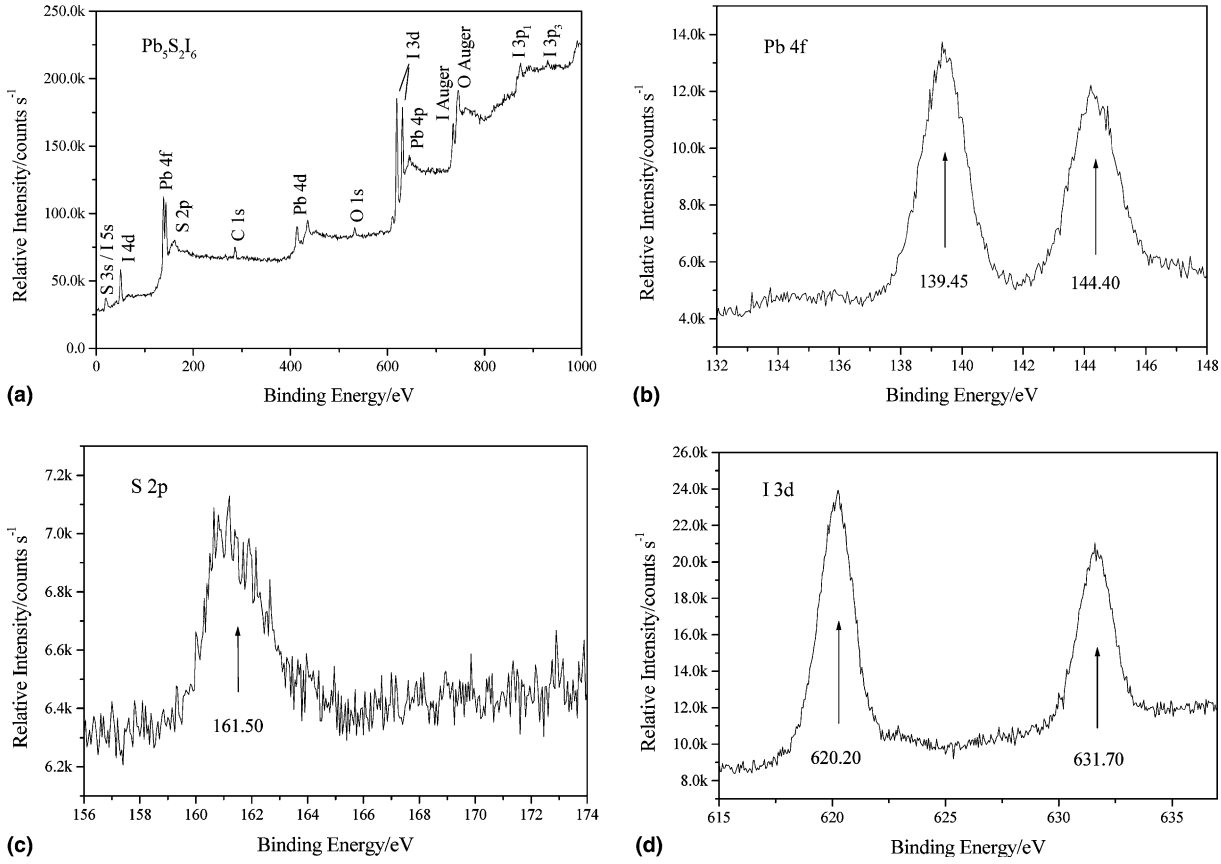

Fig. 3. XPS analysis of the as-produced $Pb_5S_2I_6$ crystals: (a) The survey spectra of the products. (b) The close-up Pb 4f. (c) The close-up S 2p. (d) The close-up I 3d.

relative intensities of the two peaks have changed and the peak at 62 cm^{-1} is shifted from its normal position (68 cm^{-1}). With further investigation, we could identify the PbI_2 vibrations from the spectra. The peak at 77 cm^{-1} is attributed to the Raman active mode E_g of PbI_2 [29]. The peaks at 97–118 cm^{-1} could be assigned to the optical phonon modes [30]. It is noted that the intense peak of A_{1g} at 97 cm^{-1} in PbI_2 becomes extremely weak, which may also be caused by the combination of PbS and PbI_2 in $Pb_5S_2I_6$ crystals. The shoulder peak at 125 cm^{-1}, not been assigned, may only attribute to the $Pb_5S_2I_6$ crystals. Fig. 5(b) shows the spectra for the nanowhiskers prepared in the route. The overall spectra have no obvious difference from the crystals (Fig. 5(a)). We may conclude that the nanowhiskers

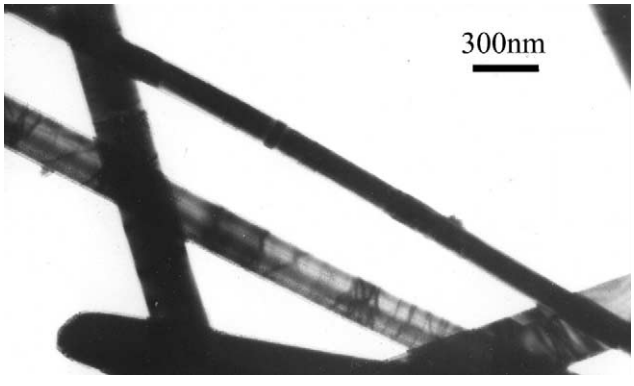

Fig. 4. TEM image of the $Pb_5S_2I_6$ nanowhiskers produced in the route.

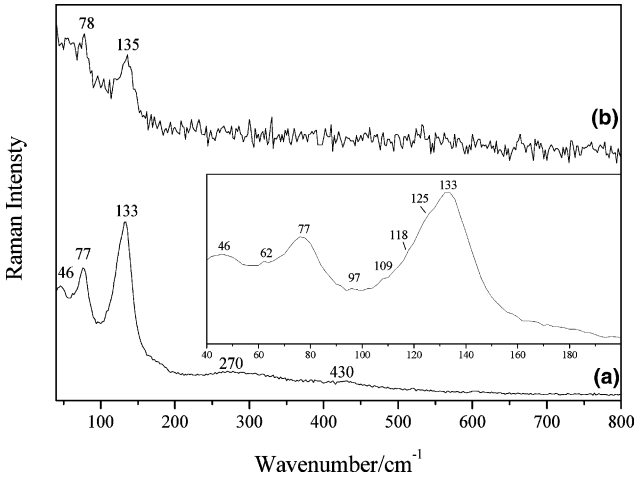

Fig. 5. Raman spectra of the samples. (a) The spectra for the as-prepared $Pb_5S_2I_6$ whiskers and tubules. The inset is the close-up spectra of the crystals from 40 to 200 cm^{-1}. (b) The spectra for the $Pb_5S_2I_6$ nanowhiskers.

have no size confinement because no peak shift was observed in the spectra.

4. Summary

In summary, $Pb_5S_2I_6$ whiskers and tubules were achieved from the moderate reaction among lead chloride, thiourea, and excess sodium iodide under hydrothermal conditions at 200 °C for 20–40 h. Meanwhile, the nanowhiskers with 50–300 nm in diameter and more than 10 μm in length were also synthesized in the route at 180–200 °C for 8–10 h. The possible mechanism and affects on the formation of the $Pb_5S_2I_6$ crystals with different size and morphologies are discussed. The Raman spectra show that the $Pb_5S_2I_6$ crystals have complex vibrational modes of PbS and PbI_2. The spectra also show that the prepared nanowhiskers have the same structure as the bulk crystals.

Acknowledgements

The project supported by Anhui Provincial Natural Science Foundation (Grant no. 3044901) and the National Natural Science Foundation of China are gratefully acknowledged. We are indebted to Prof. G.E. Zhou, C.Y. Xu, F.Q. Li, J.X. Wu, and Dr. X.M. Liu for their help in obtaining the XRD, SEM, XPS, and TEM results and the valuable comments.

References

[1] B. Reuter, K. Hardel, Angew. Chim. 72 (1960) 138.
[2] J. Fenner, A. Rabenau, Z. Anorg. Allg. Chem. 426 (1976) 7.
[3] R. Nitsche, W.J. Merz, J. Phys. Chem. Solids 13 (1960) 154.
[4] E. Fatuzzo, G. Harbeke, W.J. Merz, R. Nitsche, H. Roetschi, W. Ruppel, Phys. Rev. 127 (1962) 2034.
[5] T.M. Leonova, V.V. Sviridov, Inorg. Mater. 5 (1969) 1016.
[6] K. Takei, H. Hagiwara, H. Tanaka, Bull. Chem. Soc. Jpn. 50 (1977) 1341.
[7] J. Weissenstein, J. Horak, Czech. J. Phys. 24 (1974) 235.
[8] M. Sergent, O. Fischer, M. Decroux, C. Perrin, R. Chevrel, J. Solid State Chem. 22 (1977) 87.
[9] (a) J.D. Corbett, R.K. McMullan, D.J. Prince, Inorg. Chem. 10 (1971) 1749;
(b) A.H. Cowley, S.T. Cohen, Inorg. Chem. 3 (1964) 780.
[10] A. Ibanez, J.C. Jumas, J.O. Fourcade, E. Philippot, M. Maurin, J. Solid State Chem. 48 (1983) 272.
[11] A. Rabenan, H. Rau, G. Rosenstein, Naturwissenschaften 55 (1968) 82.
[12] A. Rabenan, H. Rau, Z. Anorg. Allg. Chem. 369 (1969) 295.
[13] Yu.M. Mininzon, V.I. Popolitov, A.N. Lobachev, Sov. Phys. Crystallogr. 22 (1977) 717.
[14] V.I. Popolitov, A.N. Lobachev, V.F. Peskin, Yu.M. Mininzon, Ferroelectrics 21 (1978) 421.
[15] V.I. Popolitov, G.F. Plakhov, Neorg. Mater. 25 (1989) 726.
[16] V.I. Popolitov, G.F. Plakhov, Neorg. Mater. 27 (1991) 2618.
[17] V.I. Popolitov, Pis'ma Zh. Tekh. Fiz. 22 (1996) 78.
[18] K. Klaus-Kurasiak, W. Wojciak, J. Signalaufzeichnungsmater 10 (1982) 105.
[19] V.F. Markov, L.N. Maskaeva, J. Anal. Chem. 56 (2001) 754.
[20] (a) J.Q. Hu, Q.Y. Lu, B. Deng, K.B. Tang, Y.T. Qian, G.E. Zhou, X.M. Liu, Inorg. Chem. Commun. (1999) 569;
(b) J. Hu, B. Deng, Q. Lu, K. Tang, R. Jiang, Y. Qian, G. Zhou, H. Cheng, Chem. Commun. (2000) 715.
[21] (a) Q. Yang, K.B. Tang, C.R. Wang, Y.T. Qian, W.C. Yu, G.E. Zhou, F.Q. Li, J. Mater. Chem. 11 (2001) 257;
(b) Q. Yang, K. Tang, C. Wang, F. Li, B. Hai, G. Shen, C. An, W. Yu, Y. Qian, J. Cryst. Growth 233 (2001) 287.
[22] C.R. Wang, K.B. Tang, Q. Yang, S.H. Lu, G.E. Zhou, F.Q. Li, W.C. Yu, Y.T. Qian, J. Cryst. Growth 226 (2001) 175.
[23] V.I. Nefedov, Y.V. Salyn, X. Keller, Zh. Neorg. Khim. 24 (1979) 2564.
[24] N.N. Sergushin, V.I. Nefedov, I.A. Rozanov, Zh. Neorg. Khim. 21 (1976) 856.
[25] M.J. Tricker, Inorg. Chem. 13 (1974) 743.
[26] B. Minceva-Sukarova, M. Najdoski, I. Grozdanov, C.J. Chunnilall, J. Mol. Struct. 410 (1997) 267.
[27] (a) K.K. Nanda, S.N. Sahu, R.K. Soni, S. Tripathy, Phys. Rev. B 58 (1998) 15405;
(b) D.T. Krauss, F.W. Wise, Phys. Rev. B 55 (1997) 9860.
[28] Y. Batonneau, C. Brémard, J. Laureyns, J.C. Merlin, J. Raman Spectrosc. 31 (2000) 1113.
[29] A. Saitoh, T. Komatsu, T. Karasawa, Phys. Rev. B 62 (2000) 11398.
[30] R. Mu, Y.S. Tung, A. Ueda, D.O. Henderson, J. Phys. Chem. 100 (1996) 19927.